Draft version January 23, 2024
Typeset using LaTeX default style in AASTeX631

Signature of high-amplitude pulsations in seven δ Sct stars via *TESS* observations

Fatemeh Vasigh [1], Elham Ziaali [1] and Hossein Safari [1,2]

[1] *Department of Physics, Faculty of Science, University of Zanjan, University Blvd., Zanjan, 45371-38791, Zanjan, Iran*
[2] *Observatory, Faculty of Science, University of Zanjan, University Blvd., Zanjan, 45371-38791, Zanjan, Iran*

ABSTRACT

The regular behavior of the pulsations of high-amplitude δ Sct (HADS) stars gives a greater chance to investigate the interiors of stars. We analyzed seven HADS stars showing peak-to-peak amplitudes of more than 0.3 mag that were newly observed by *TESS*. We obtained that TIC 374753270, TIC 710783, and TIC 187386415 pulsate in fundamental radial mode, also, TIC 130474019 and TIC 160120432 show double radial modes. However, TIC 148357344 and TIC 278119167 demonstrate triple-mode behavior. Our analysis shows that these seven stars are close to the red edge of the instability strip in the Hertzsprung-Russell (HR) diagram, quite into the δ Sct stars range. The fundamental mode of these seven targets follows the period-luminosity (PL) relation for δ Sct stars. However, TIC 278119167 deviates slightly from the fundamental PL relation. The double-mode and triple-mode HADS stars (TIC 130474019, TIC 160120432, TIC 148357344, and TIC 278119167) well cover the period ratio ranges (fundamental to first and second overtones). Using the information of 176 HADS stars (Netzel and Smolec), we find a scaling relation ($[\mathrm{Fe/H}] \propto \log(M^{7.95}L^{-1.83}\mathrm{P0}^{0.79}\mathrm{T}_{\mathrm{eff.}}^{0.047})$) between the metallicity ([Fe/H]) and mass (M), luminosity (L), effective temperature (T_{eff}), and the fundamental period (P0). We estimate the metallicity of the seven newly identified HADS stars ranging from -0.47 dex to 0.28 dex.

Keywords: Asteroseismology (73); Delta Scuti variable stars (370); Stellar oscillations (1617)

1. INTRODUCTION

Asteroseismology is an approach to studying the internal characteristics of pulsating stars through their oscillation modes (Aerts et al. 2010; Antoci et al. 2019; Bedding et al. 2020; Holdsworth et al. 2024). The asteroseismology approach has more detailed explanations for the interior structure of different stars, with increasing the resolution of ground and space observations of the pulsating stars. Studies of *Kepler* (Gilliland et al. 2010) data have had the essential impacts on asteroseismology. Recently, the Transiting Exoplanet Survey Satellite (*TESS*, Ricker et al. (2015)) provides unprecedented qualified space observations of numerous star systems. Antoci et al. (2019) reported the information of 117 δ Sct stars from *TESS* short cadence observations for sectors 1 and 2. Very recently, Read et al. (2024) identified 848 δ Sct stars having a narrow color range of $0.29 < G_{BP} - G_{RP} < 0.31$ (at the center of instability strip) and are nearer than 500 pc, by using sectors 27-55 of *TESS* observations and *Gaia* DR3 information. Investigating the pulsation property of δ Sct stars could help to understand their internal structure, such as rotation, chemical composition, density, temperature, and gravity.

In the Hertzsprung-Russell (HR) diagram, δ Sct stars are pulsating variables of spectral types A0-F5 that mainly lie at the overlapping of the main sequence and the instability strip (Breger 1979; Murphy et al. 2020; Bowman & Michielsen 2021). The δ Sct stars have the intermediate mass located at the transition region from low-mass to high-mass stars. Stars with lower than one and higher than two solar masses are called low-mass and high-mass, respectively. The effective temperature range of the δ Sct stars lies between 6500 K to 9500 K (Petersen & Christensen-Dalsgaard 1996; Breger 2000a; McNamara 2011; Bowman et al. 2016; Pietrukowicz et al. 2020; Murphy et al. 2019; Jayasinghe et al. 2020; Yang et al. 2021b). The δ Sct stars pulsation frequencies are in the range of $5 - 80\,\mathrm{d}^{-1}$. They show various modes of pulsations such as radial, non-radial pressure modes, and

Corresponding author: Elham Ziaali, Hossein Safari
ziaali@znu.ac.ir
safari@znu.ac.ir

mixed modes of the low radial order in their complex light curves (Houdek et al. 1999; Breger 2000b; Handler 2009; Hasanzadeh et al. 2021; Soszyński et al. 2021)

Their pulsations are primarily driven by the classical κ mechanism in the He II ionization zone. Some studies also suggested that intrinsically stable stochastically driven (solar-like) p modes may be excited simultaneously in such δ Sct star (Baker & Kippenhahn 1962; Balmforth & Gough 1990; Houdek et al. 1999; Samadi et al. 2002; Antoci et al. 2011; Antoci 2014).

High-amplitude δ Sct (HADS) stars pulsate in V-band amplitudes over 0.3 mag. HADS stars are characterized by their high amplitude, short periods (on the order of hours), and also $v \sin i \leq 30$ kms^{-1}. HADS stars oscillate as single-periodic with a radial fundamental mode or double- or triple-periodic pulsators (Bono et al. 1997; Wils et al. 2008; McNamara 2011; Yang et al. 2021a; Netzel & Smolec 2022; Lv et al. 2023; Xue et al. 2023). However, the number of HADS stars having four independent radial frequencies as quadruple-mode HADS stars has been increasing in recent years (Mow et al. 2016; Lv et al. 2022).

Also, non-radial modes may exist in the HADS frequency spectrum (Uytterhoeven et al. 2011). Modes in the high-amplitude pulsations of HADS stars are driven by e.g., the κ mechanism. HADS stars are important because they can be used to study the structure and evolution of stars. These stars can be used to investigate the evolution of stellar populations, as they are found in old stellar populations, while, low amplitude δ Sct (LADS) stars are young and intermediate age stars (Chang et al. 2013; Netzel & Smolec 2022; Soszyński et al. 2021). Recently, there has been a growing interest in HADS stars as potential targets for exoplanet searches. High-precision observations of HADS stars' pulsations and signatures of orbiting planets could detect slight variations in their light curves. Several exoplanets have already been discovered around HADS stars (Hey et al. 2021; Guzik 2021). Lv et al. (2023) studied seven new HADS stars through photometric data of *TESS*, and reported that two stars may be RR Lyraee based on their light curves and the difference in their placement with the HADS star in the Peterson and period-luminosity (PL) diagram. In these HADS stars, the metallicity can have a greater effect than the rotation of the star on the period ratios, as the ratio of overtones to fundamental decreases with increasing metallicity.

Metallicity is often expressed as a ratio of the abundance of iron (Fe) to hydrogen (H) compared to the solar ratio, written as [Fe/H] (Kotoneva et al. 2002; Chruslinska & Nelemans 2019). A metallicity value greater than -0.5 dex indicates metal-rich δ Sct stars, while a value less than -1.5 dex shows a metal-poor star (McNamara 2011). Determining a star's metallicity involves sophisticated astronomical techniques based on spectroscopic investigations (Lianou et al. 2011; Liu et al. 2020), photometric methods (Li et al. 2023; Dékány & Grebel 2022) and astroseismology approach (Netzel & Smolec 2022). Here, we analyzed the light curves of seven newly identified HADS stars from *TESS* observations. To do this, we extracted the frequencies and amplitudes of these seven stars using the periodogram analysis.

We studied the PL behaviour and HR diagram. To determine the metallicity of targets, we obtained a scaling relation between the metallicity of 176 HADS stars (Netzel & Smolec 2022) and their physical parameters (mass, luminosity, and effective temperature) and the fundamental periods. Section 2 gives the HADS star information used in this paper. Sections 3 and 4 explain the methods and results, respectively. Finally, section 5 summarises the essential findings of the present work.

2. DATA

TESS is a space mission for probing exoplanets (Ricker et al. (2015)). This telescope divides the sky into 26 sectors and observes each sector for 27 days. *TESS* space telescope designed to record objects in a red filter of approximately 600–1000 nm (Aguirre et al. 2015; Barclay et al. 2018). *TESS* data is available in two forms, target pixel file (TPF) and light curve, which can be searched applying the Lightkurve tool (Lightkurve Collaboration et al. 2018). Figure 1 illustrates target pixel file and aperture (red squares) for TIC 374753270 (left-top row panel), TIC 130474019 (right-top row panel), TIC 148357344 (left-middle row panel), TIC 160120432 (right-middle row panel), TIC 278119167 (left-bottom row panel), TIC 710783 (right-bottom row panel), and TIC 187386415 (bottom-row panel). As shown in the figure, each aperture covers the primary pixels of each target without considerable contamination of another object in field-of-view. In this paper, we used photometric data processed by SPOC (Jenkins et al. 2016), which are short cadence (2 min). We transformed the flux to magnitude and subtracted from its average value for each light curve to get the corrected time series. We investigated the flux of seven δ Sct stars to find high-amplitude pulsations and peak-to-peak amplitudes more significant than 0.3 mag, a criterion for being a HADS. Table 1 tabulates information on seven newly recognized HADS stars. The table includes the name, sector(s), length of data light curve, and observation duration of targets.

3. METHOD

3.1. *Frequency analysis*

We selected seven δ Sct light curves (related to TPFs of Figure 1) with peak-to-peak amplitudes greater than 0.3 mag as an essential characteristic for identifying HADS stars. Then, their light curves were analyzed to extract pulsation frequencies. However, there

Table 1. TIC number, variable name, and *TESS* short cadence sector(s) for seven HADS stars.

TIC	Star name	Sector
374753270	-	36,37
130474019	-	7, 34
148357344	-	7
160120432	YZ UMi	14, 19, 20, 40, 47, 52, 53
278119167	-	40, 53
710783	-	5
187386415	-	51

are few reports on HADS stars showing the peak-to-peak value slightly smaller than 0.3 mag (Breger et al. 2011; Lv et al. 2023). We first removed outliers from each star's light curve. We dropped the data points with values more significant than four standard deviations (4σ) as the outliers of the light curves. Also, the mean of each single light curve was subtracted to get the corrected systematic error flux.

We constructed a light curve for each TPF to correspond with the SPOC-prepared light curve to ensure the validity of the signal-to-noise ratio. To study our samples' pulsating behavior, the PERIOD04 (Lenz & Breger 2005) software was applied. A pre-whitening procedure carries out the frequency extraction. The Nyquist frequency is half of the sampling rate, f_N = 360.048 d^{-1} for 2-minute cadence observations. This value is well above the limit range ($3 < f < 80$ d^{-1}) expected for a typical δ Sct star pulsation. We used a resolution frequency $f_{res} = 1.5/\Delta T$ to identify nearby frequencies in the power spectrum, where ΔT represents the length of light curve (Loumos & Deeming 1978). Two frequencies are resolved if the frequency difference is more significant than the resolution frequency. The light curves are modeled by:

$$m = m_0 + \Sigma_{i=1}^{N} A_i \sin(2\pi(f_i t + \phi_i)), \quad (1)$$

where m_0 is the zero point, A_i is the amplitude, f_i is the frequency, and ϕ_i is the phase. The basis of PERIOD04 is to recognize the considerable peaks as important frequencies.

When all the essential frequencies are identified, multi-frequency modeling (Equation 1) via the least-squares approach of the light curve is performed. Then, the PERIOD04 algorithm gives frequency, amplitude, and phase for each mode. Finally, the residual is determined by subtracting each mode from the original light curve. We considered the modes with a signal-to-noise ratio (SNR) more significant than 5.2 (Baran et al. 2015). This procedure is repeated until the recognition the all essential modes. The final residual is expected to show the lack of considerable modes (SNR> 5.2). The uncertainty of the frequencies is determined using the approach by Montgomery & O'Donoghue (1999).

3.2. *Asteroseismic analysis*

The stellar oscillations are helpful to infer information about the stars' interior. Each mode contains three quantum numbers: n (radial number), l (degree), and m (azimuthal number), that are related to the characteristics of oscillations. In most pulsating stars, we expect the highest amplitude to be related to the fundamental radial ($n = 1, l = 0$) oscillation (Aerts et al. 2010; Murphy et al. 2020).

The δ Sct stars' power spectrum, the frequency corresponding to the highest peak amplitude, is called $f_{A_{max}}$. The $f_{A_{max}}$ might change over time due to modulation of amplitude and other factors such as noise (Bowman 2017). Radial modes can be identified based on the ratio of their periods. Period ratios for radial modes (fundamental (F0), first (F1), second (F2) and third (F3) overtones) were first presented by Stellingwerf (1979) based on theoretical models as F0/F1 = 0.756_ 0.787, F0/F2 = 0.611_ 0.632, and F0/F3 = 0.50_ 0.525.

For δ Sct stars with the first and the second overtones, the characteristic period ratios are around F1/F2 = 0.8 (Soszyński et al. 2021). The combination of different frequencies or the linear sum of the independent frequencies, $n\nu_i \pm m\nu_j$, were identified by Loumos & Deeming (1978) criteria. The modes with no agreement with combination or harmonic frequencies might be identified as non-radial modes. Whereas the frequency (period) of pulsations is linked to stars' interior characteristics, the frequency is related to the radius changes. The critical factor is the density of stars that is accurately related to the period. The period-density

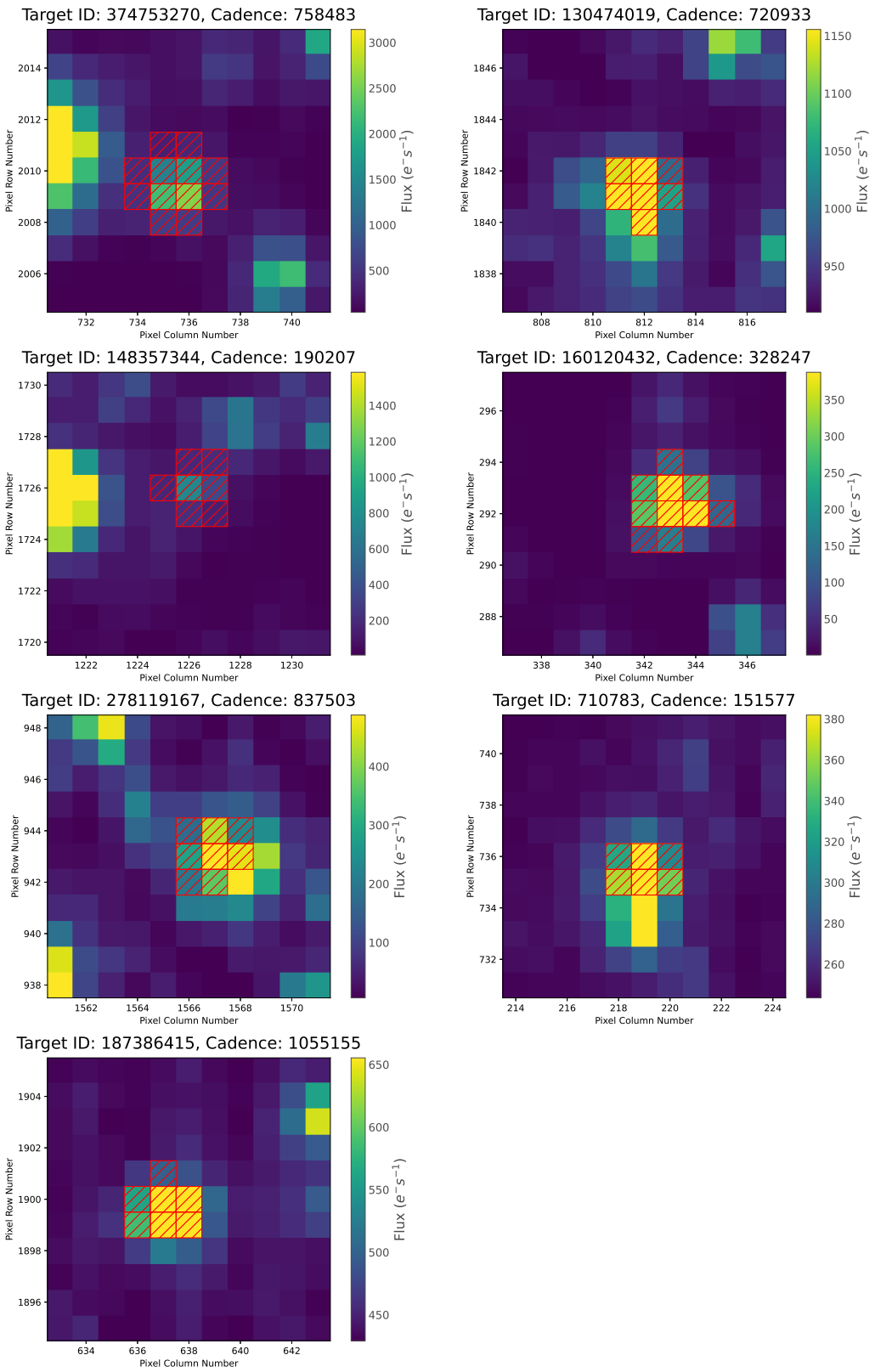

Figure 1. Target Pixel File (TPF) for TIC 374753270 (left-first row), TIC 130474019 (right-first row), TIC 148357344 (left-second row), TIC 160120432 (right-second row), TIC 278119167 (left-third row), TIC 710783 (right-third row), and TIC 187386415 (fourth-row). The aperture for each target star is indicated by the red squares.

relation defines as,

$$Q = P\sqrt{\overline{\rho}/\overline{\rho}_{\odot}}, \tag{2}$$

where $\overline{\rho}$ describes the mean densities of the target star and $\overline{\rho}_{\odot}$ is the mean density for Sun. P is the pulsation period. The other forms of Equation (2) were given by Breger (1990) that included the gravity acceleration and bolometric magnitudes. Here, we used Equation (2) to validate the periods of seven targets. The range of pulsations constant (Q) for δ Sct stars' fundamental, first, second, and third overtone frequencies are 0.027_ 0.04, 0.021_ 0.027, 0.018_ 0.021, and 0.016_ 0.017, respectively (Breger & Bregman 1975; Milligan & Carson 1992).

3.2.1. *Period-Luminosity relation*

The period-luminosity (PL) relation is a dependency between the star's luminosity and density. Consequently, this relation occurs between the luminosity and the pulsation period of a group of pulsating stars that have a relatively narrow range of effective temperature. The PL relation was given by Leavitt & Pickering (1912). We computed the absolute V-band magnitudes ($M_{\rm V}$) for our seven targets using the following Equation,

$$M_{\rm V} = m_{\rm v} + 5\log\pi + 5 - A_{\rm V}, \tag{3}$$

where $m_{\rm v}$ is the apparent magnitude in the V-band and π denotes the star's parallax (in arcsec) collected from *Gaia* DR3. Since interstellar dust can impact the flux of stars (luminosity), the $M_{\rm V}$ values were corrected for extinction ($A_{\rm V}$). Following Green et al. (2018), we determined the extinction for our seven targets to correct the V-band magnitudes. All seven samples have fractional parallax uncertainties (the ratio of parallax uncertainty to the parallax) smaller than 0.05 and extinctions less than 0.6. By applying the Tycho V_T and B_T magnitudes, we calculated the Johnson V apparent magnitudes as, (199 1997),

$$V = V_T - 0.090(B_T - V_T). \tag{4}$$

We investigated the validity of the obtained fundamental frequencies by using the PL relation for our targets. Using *Gaia* DR2 parallaxes Ziaali et al. (2019) gave the PL relation for δ Sct stars observed by *Kepler*, as follows,

$$M_{\rm V} = (-2.94 \pm 0.06)\log(P) + (-1.34 \pm 0.06), \tag{5}$$

While Barac et al. (2022) reported a similar relation for stars observed by *TESS* using the *Gaia* DR3 parallaxes,

$$M_{\rm V} = (-3.01 \pm 0.07)\log(P) + (-1.40 \pm 0.07). \tag{6}$$

Also, using multi-colour photometric ground-based observations, Poro et al. (2021) gave,

$$M_{\rm V} = (-3.200 \pm 0.010)\log(P) - (1.599 \pm 0.010). \tag{7}$$

By using Equation 3 the absolute magnitude for each single star was calculated and the PL diagram is examined (Section 4.8). These PL relations Equations (5-6-7) are very close together in a narrow ridge for δ Sct stars. So, the magnitudes and fundamental periods should be consistent with the PLs within the observational uncertainties.

4. RESULTS

To identify the HADS stars, we applied harmonic analysis and asteroseismology for δ Sct targets through observations by *TESS*. We expected the HADS light curves to show a peak-to-peak amplitude more significant than 0.3 mag. For each case, we examined the harmonic analysis to study the properties of the power spectrum. We considered the frequencies with SNR > 5.2 to ensure the validity of the identified frequencies. We obtained the period ratio, Q value, and large frequency separation. We applied the PL relation as the final criteria for the fundamental radial mode of our seven newly recognized HADS stars (Table 1).
Figure 2 displays the position of the seven HADS stars (colored star markers) between the instability strip edges in the HR diagram given by Murphy et al. (2019). As displayed in the figure, these seven targets tend toward the instability strip's red edge with lower temperatures. Murphy et al. (2019) investigated the instability strip boundaries based on the position of 15000 δ Sct stars in the *Kepler* field-of-view using TDC and mixing length (α_{MLT}=1.8) reported by Dupret et al. (2005). In the remainder of this paper, we examined the HADS star criteria for these seven targets.

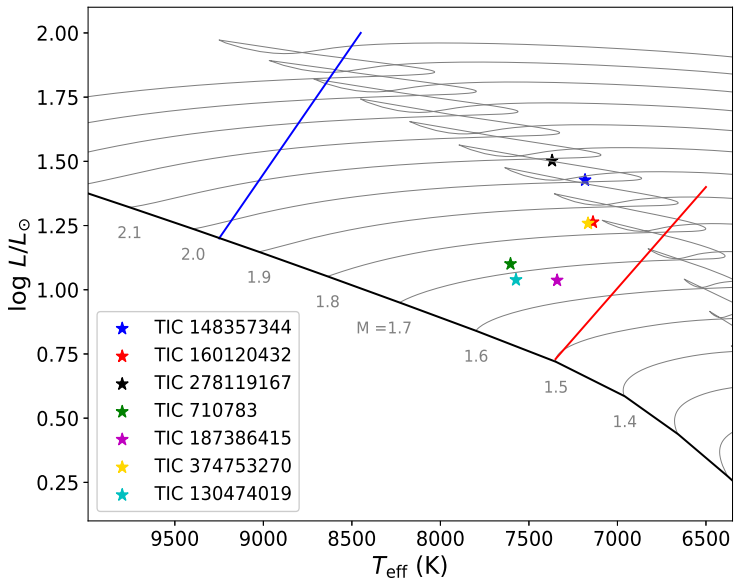

Figure 2. HR diagram including our seven HADS stars indicated with different colored star markers. The observational red and blue edge of the instability strip for δ Sct stars along with the evolutionary tracks with $X = 0.71$, $Z = 0.014$, and α_{MLT}=1.8 were obtained by Murphy et al. (2019).

4.1. *TIC 374753270*

Figure 3 represents the light curve (top panel), power spectrum (middle panel), and power spectrum's residuals (bottom panel) for TIC 374753270 (TYC 8943-3384-1) star. Barac et al. (2022) introduced TIC 374753270 ($RA = 10^h03^m20.620266^s$, $DE = -61^h51^m15.63198^s$) as a δ Sct star. We analyzed sector 36 with a duration of 23.44 days and consisting of 17171 data points. By harmonic analysis of the light curve, we detected 14 acceptable frequencies. The frequencies are listed in the Table 2, including one independent frequency (mono-mode HADS) of F0 = 7.245 d^{-1} (P0 = 0.138 days). Other frequencies might be called harmonics (f_2, f_3, f_4, f_5, f_7, f_8) and non-radial modes (f_6, f_9, ..., f_{14}). These frequencies are in the reported range for δ Sct stars (Breger 2000a; Liakos & Niarchos 2017). However, in some studies, this range was restricted to greater than 5 d^{-1} (Murphy et al. 2019). Removing these 14 identified modes, we obtained the power spectrum's residual that indicated the absence of significant modes with SNR greater than 5.2. The Q value of the radial fundamental mode is 0.032, which is quite into the reported range of fundamental mode for δ Sct stars. The rectified light curve shows a peak-to-peak amplitude of about $\sim$ 0.43 mag, which is slightly more than 0.3 mag (expected for HADS stars).

4.2. *TIC 130474019*

Figure 4 shows the light curve (top panel), power spectrum (middle panel), and power spectrum's residuals (bottom panel) for TIC 130474019 (TYC 7636-1969-1) star. Barceló Forteza et al. (2020) determined the physical parameters (temperature, gravity, and frequency scaling relation) of TIC 130474019 ($RA = +18^h38^m50.4^s$, $DE = +19^h07^m44.6^s$) using *TESS* observation, while Barac et al. (2022) introduced this star as a δ Sct sample. This star's light curve recorded in sector 34 includes 16850 data points. Table 3 shows the seven frequencies, which include two independent frequencies of F0 = 12.282 d^{-1} (fundamental, P0 = 0.0814 days) and F1 = 15.89 d^{-1} (first overtone) with Q values as 0.04 and 0.031 respectively. The frequency ratio (F0/F1) is obtained to be 0.78, which indicates the independent property and validity of the fundamental and first overtone. As tabulated in table3, we observed the harmonics frequencies (f_2, f_3, f_4), combination frequencies (f_6, f_7), and non-radial modes (f_8,...,f_{12}). The peak-to-peak amplitude is about $\sim$ 0.3 mag and the range of the frequencies that might be suggested TIC 130474019 as a double-mode HADS star.

4.3. *TIC 148357344*

Figure 5 displays the light curve (top panel), power spectrum (middle panel), and power spectrum's residuals (bottom panel) for TIC 148357344 (TYC 5968-1693-1) star. TIC 148357344 ($RA = +07^h05^m28.9^s$, $DE = -17^h05^m16.8^s$) was first identified as a

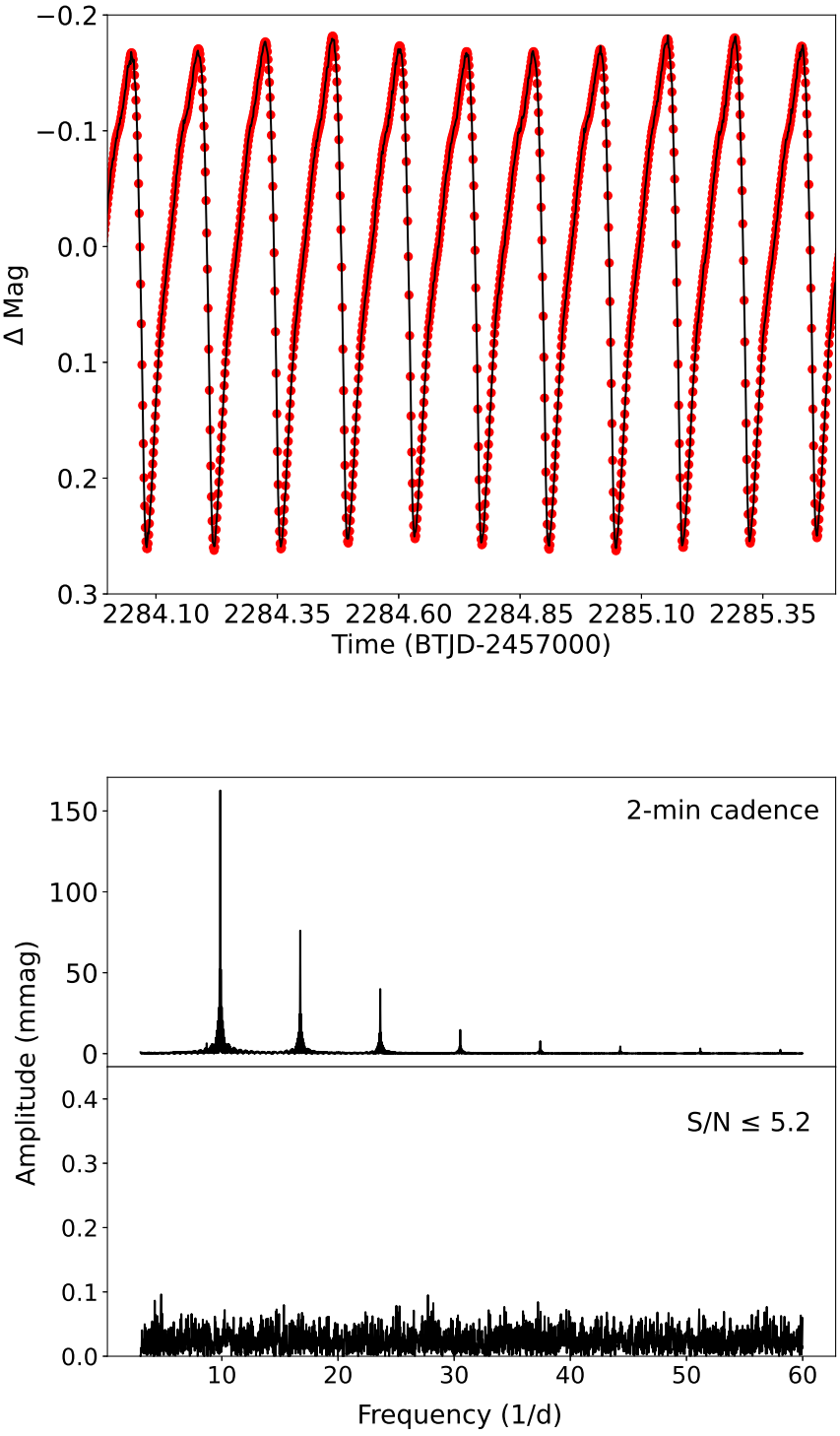

Figure 3. The short cadence light curve of TIC 374753270 during 1.5 days (top panel), power spectrum (middle panel), and power spectrum's residuals with SNR less than 5.2 (bottom panel).

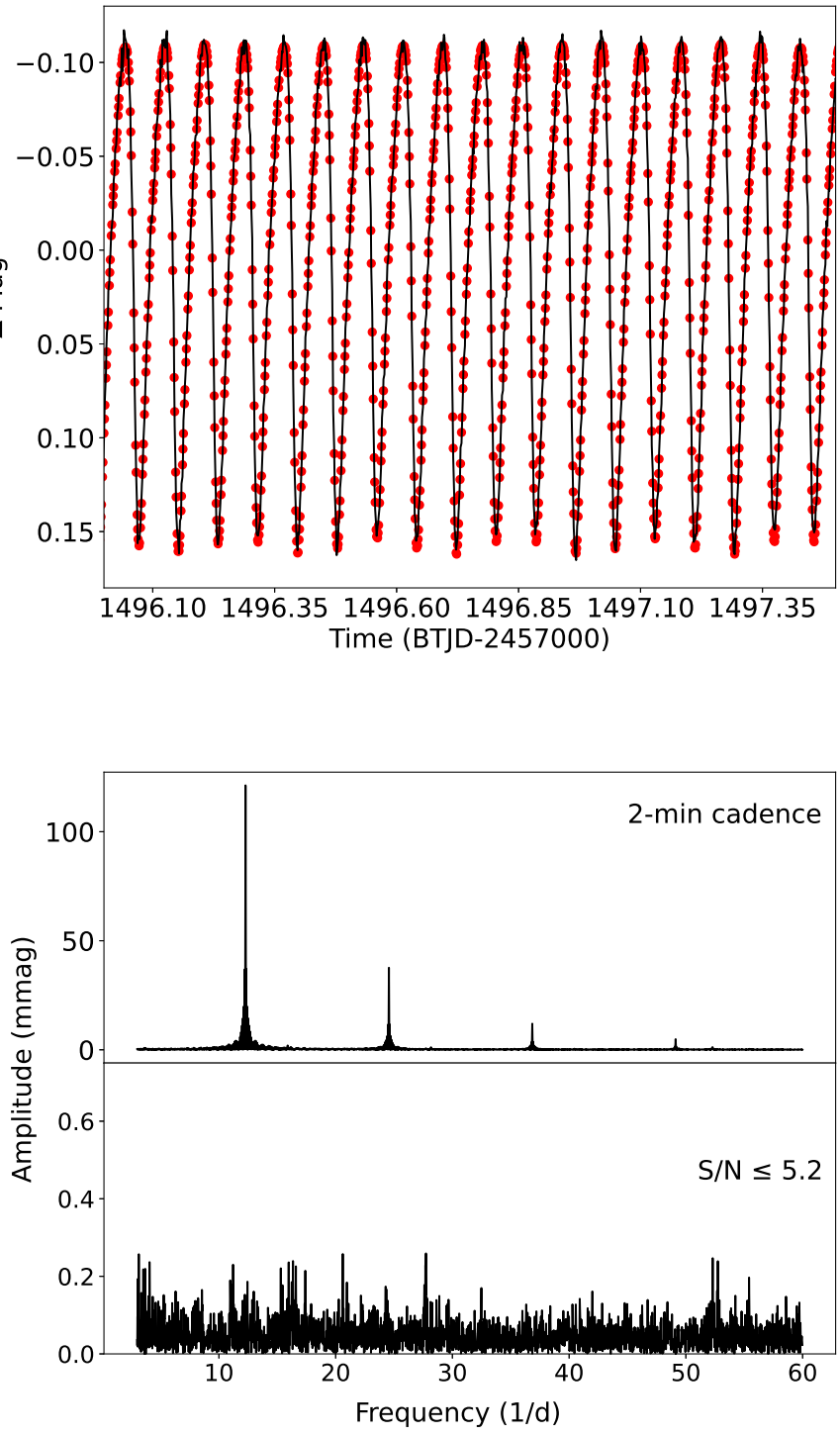

Figure 4. The short cadence light curve of TIC 130474019 during 1.5 days (top panel), power spectrum (middle panel), and power spectrum's residuals with SNR less than 5.2 (bottom panel).

Table 2. A complete list of the 14 frequencies identified TIC 374753270 (denoted by f_i). The frequency resolution is about f_{res} = 0.0618.

f_i	Frequency (d^{-1})	Amplitude (mmag)	phase (radians)	S/N	ID	period ratio	Q value
1	7.245±0.000004	162.557±0.03	0.700±0.0003	721.07	F0	-	0.032±0.004
2	14.491±0.00001	76.138±0.03	0.316±0.0007	765.7	2F0	-	-
3	21.737±0.00002	40.11±0.03	0.953±0.0001	903.144	3F0	-	-
4	28.984±0.00005	14.84±0.03	0.488±0.0003	444.856	4F0	-	-
5	36.229±0.0001	7.988±0.03	0.566±0.0007	251.143	5F0	-	-
6	6.014±0.0001	5.849±0.03	0.738±0.0009	181.028	-	-	-
7	43.476±0.0001	4.556±0.03	0.696±0.001	170.851	6F0	-	-
8	50.721±0.0002	3.856±0.03	0.467±0.001	106.987	7F0	-	-
9	57.968±0.0003	2.943±0.03	0.497±0.002	74.838	-	-	-
10	12.028±0.0005	1.352±0.03	0.630±0.004	19.987	-	-	-
11	3.007±0.001	0.599±0.03	0.336±0.009	15.07	-	-	-
12	18.044±0.001	0.531±0.03	0.698±0.01	17.45	-	-	-
13	13.261±0.001	0.452±0.03	0.991±0.01	15.06	-	-	-
14	8.47±0.003	0.206±0.03	0.726±0.02	6.42	-	-	-

Table 3. A complete list of the 12 frequencies identified TIC 130474019 (denoted by f_i). The frequency resolution is about f_{res} = 0.06.

f_i	Frequency (d^{-1})	Amplitude (mmag)	phase (radians)	S/N	ID	period ratio	Q value
1	12.282±0.00001	121.255±0.06	0.984±0.00008	1249.2	F0	-	0.04±0.004
2	24.564±0.00003	37.73±0.06	0.926±0.0002	618.58	2F0	-	-
3	36.846±0.0001	11.96±0.06	0.780±0.0008	262.86	3F0	-	-
4	49.129±0.0002	4.92±0.06	0.698±0.002	111.06	4F0	-	-
5	15.890±0.0007	1.945±0.06	0.026±0.005	21.60	F1	0.78	0.027±0.003
6	28.173±0.001	1.175±0.06	0.925±0.008	18.25	F0+F1	-	-
7	3.611±0.001	0.949±0.06	0.914±0.01	10.05	F1-F0	-	-
8	15.41±0.002	0.638±0.06	0.815±0.01	8.15	-	-	-
9	16.01±0.002	0.609±0.06	0.023±0.01	8.57	-	-	-
10	8.672±0.002	0.471±0.06	0.672±0.02	9.00	-	-	-
11	40.452±0.002	0.468±0.06	0.897±0.02	9.03	-	-	-
12	28.299±0.003	0.419±0.06	0.492±0.02	7.13	-	-	-

variable star by Heinze et al. (2018), then it was introduced as δ Sct by Barac et al. (2022). TIC 148357344 was observed only in sector 7 (short cadence) with a duration of 27 days and consisting of 16056 data points. We identified 12 frequencies for this star (Table 4), which includes three independent frequencies F0 = 8.36 d^{-1} (P0 = 0.119 days), F1 = 11.099 d^{-1} and F2 = 13.835 d^{-1}, as fundamental, first, and second overtones, respectively. The frequency ratios for the first (F0/F1) and the second (F0/F2) overtones were obtained as 0.76 and 0.61, respectively, determining the validity of our analysis along with the Q values as 0.028, 0.023, and 0.018 for fundamental, first, and second overtones, respectively. Other frequencies may be known as harmonics (f_2, f_3,..., f_5), combination frequencies (f_7, f_8, f_{10}), and non-radial modes (f_{11},f_{12}). It is noticeable that the first overtone's amplitude is more significant than that of the fundamental mode, probably owing to amplitude modulation mechanisms that are well-known in δ Sct stars (Bowman et al. 2016; Lv et al. 2021; Sun et al. 2021). Consequently, further studies are necessary to illuminate the driving mechanisms, including the mode selecting processes in δ Scts. The light curve's peak-to-peak value of about ~ 0.4 mag and the range of frequencies propose that TIC 148357344 may be a triple-mode HADS.

4.4. *TIC 160120432*

Figure 6 shows the light curve (top panel), power spectrum (middle panel), and power spectrum's residuals (bottom panel) for TIC 160120432 (TYC 4638-455-1) star. Using NSVS and ASAS-3 databases, Otero (2007) suggested TIC 160120432 ($RA = +15^h35^m30.4^s$, $DE = +85^h37^m38.9^s$) as HADS star. We have chosen sector 14 with a duration of 25 days and 18424 data points. In Table 5, we found 20 frequencies for TIC 160120432, which include three independent frequencies F0 = 10.350

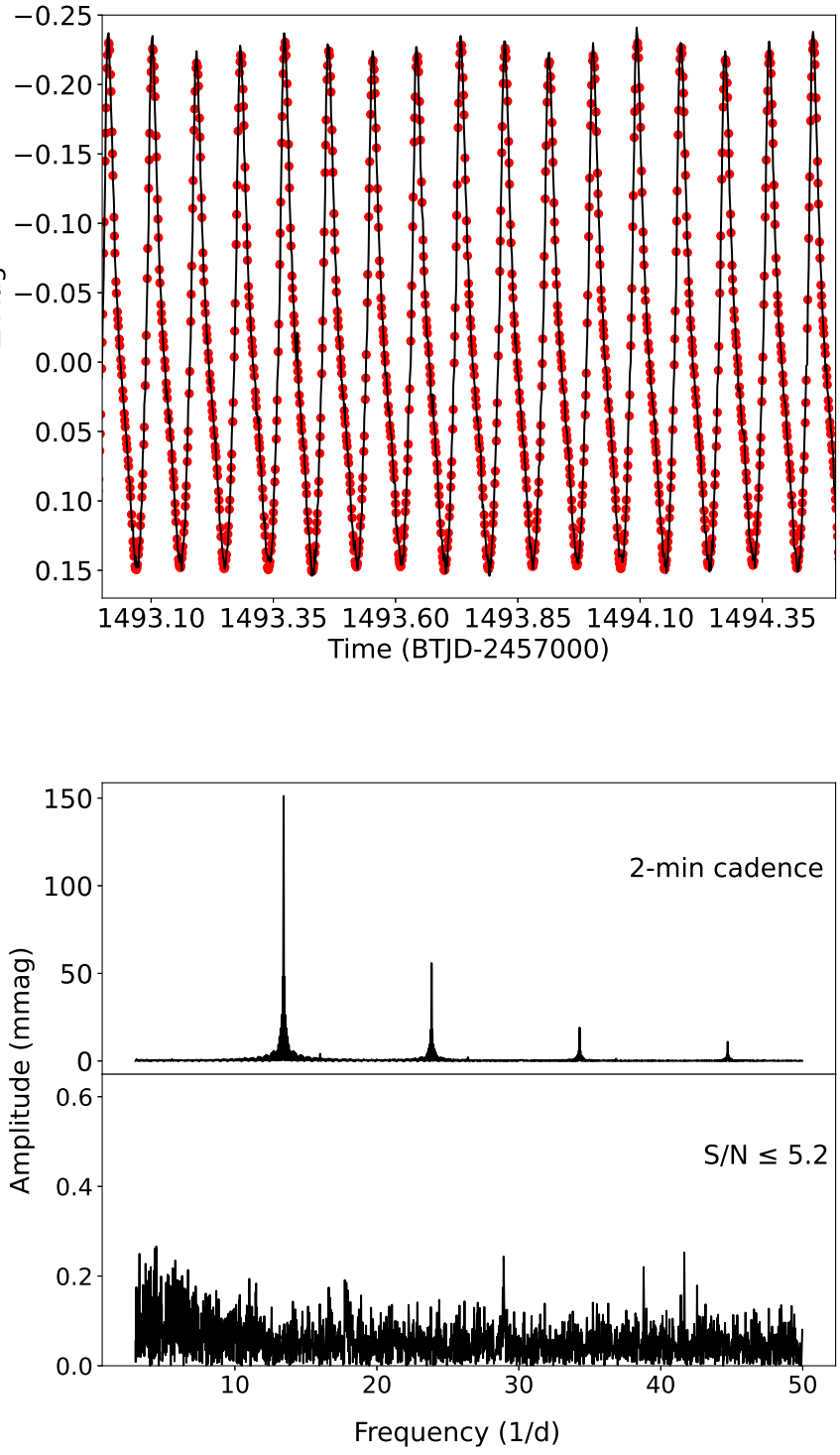

Figure 5. The short cadence light curve of TIC 148357344 during 1.5 days (top panel), power spectrum (middle panel), and power spectrum's residuals with SNR less than 5.2 (bottom panel).

Table 4. A complete list of the 13 frequencies identified TIC 148357344 (denoted by f_i). The frequency resolution is about f_{res} = 0.061.

f_i	Frequency (d^{-1})	Amplitude (mmag)	phase (radians)	S/N	ID	period ratio	Q value
1	11.09±0.00001	151.003±0.08	0.96±0.00009	1948.012	F1	0.76	0.023±0.003
2	22.19±0.00003	55.44±0.08	0.32±0.0002	942.301	2F1	-	-
3	33.29±0.00009	19.09±0.08	0.60	334.345	3F1	-	-
4	44.39±0.0001	10.92±0.08	0.84±0.0007	198.396	4F1	-	-
5	55.49±0.0006	6.72±0.08	0.48±0.001	134.900	5F1	-	-
6	13.83±0.001	2.93±0.08	0.59±0.004	55.0831	F2	0.61	0.018±0.002
7	24.93±0.001	1.85±0.08	0.42±0.007	34.443	F1+F2	-	-
8	47.13±0.003	0.56±0.08	0.67±0.01	11.070	3F1+F2	-	-
9	8.43±0.003	0.51±0.08	0.98±0.02	12.999	F0	-	0.028±0.004
10	58.23±0.003	0.44±0.08	0.29±0.02	11.216	3F1-F2	-	-
11	30.55±0.004	0.39±0.08	0.61±0.003	9.018	-	-	-
12	19.46±0.004	0.38±0.08	0.71±0.003	6.32	-	-	-

Table 5. A complete list of the 20 frequencies identified TIC 160120432 (denoted by f_i). The frequency resolution is about f_{res} = 0.055.

f_i	Frequency (d^{-1})	Amplitude (mmag)	phase (radians)	S/N	ID	period ratio	Q value
1	10.350±0.000008	126.46±0.05	0.213±0.00006	833.92	F0	-	0.031±0.00323
2	20.701±0.00002	50.991±0.05	0.400±0.0001	332.078	2F0	-	-
3	31.052±0.00005	21.50±0.05	0.394±0.0003	189.650	3F0	-	-
4	41.402±0.0001	10.378±0.05	0.710±0.0008	134.024	4F0	-	-
5	51.753±0.0002	4.86±0.05	0.051±0.001	89.726	5F0	-	-
6	9.678±0.0009	1.167±0.05	0.503±0.007	14.46	-	-	-
7	19.579±0.001	0.956±0.05	0.833±0.008	8.817	-	-	-
8	16.161±0.0009	1.069±0.05	0.641±0.007	9.713	-	-	-
9	18.847±0.0002	0.912±0.05	0.754±0.002	28.526	-	-	-
10	13.618±0.001	0.694±0.05	0.837±0.01	8.880	F1	0.76	0.023±0.003
11	29.929±0.001	0.625±0.05	0.249±0.01	8.064	-	-	-
12	9.236±0.001	0.546±0.05	0.626±0.01	9.467	-	-	-
13	26.510±0.002	0.524±0.05	0.745±0.01	9.585	-	-	-
14	40.280±0.002	0.487±0.05	0.836±0.01	7.792	-	-	-
15	19.642±0.002	0.555±0.05	0.416±0.01	7.618	-	-	-
16	40.062±0.002	0.511±0.05	0.167±0.01	8.130	-	-	-
17	19.407±0.001	0.539±0.05	0.876±0.01	7.772	-	-	-
18	30.380±0.002	0.458±0.05	0.680±0.01	7.127	-	-	-
19	15.518±0.002	0.435±0.05	0.238±0.01	7.35875	-	-	-
20	18.888±0.0003	0.531±0.05	0.280±0.02	8.329	-	-	-

d^{-1} (P0 = 0.0966 days) and F1 = 13.618 d^{-1}, with Q values as 0.031 and 0.023 respectively. As shown in Table5, We specified the harmonic frequencies (f_2, f_3,..., f_5) and non-radial modes (f_6, f_7,f_8, f_9, f_{11}, f_{12}..., f_{20}). The light curve's peak-to-peak value is about ~ 0.33 mag. The frequencies of TIC 160120432 is ranging from 9 to 51. The frequency ratio (F0/F1) is 0.76, and the Q values were calculated as 0.031 and 0.024 for the fundamental and first overtone, respectively. These four findings strongly verified the HADS property for TIC 160120432 as a new double-mode HADS star.

4.5. *TIC 278119167*

Figure 7 represents the light curve (top panel), power spectrum (middle panel), and power spectrum's residuals (bottom panel) for TIC 278119167 (TYC 1578-1754-1) star. TIC 278119167 ($RA = +14^h14^m41.2^s$, $DE = -61^h44^m57.0^s$) was categorized by Heinze et al. (2018) in the variable star catalog. This investigation indicates that TIC 278119167 is triple-mode HADS. We analyzed sector 40 with a duration of 25 days and consisting of 19611 data points. We identified 9 frequencies constructing

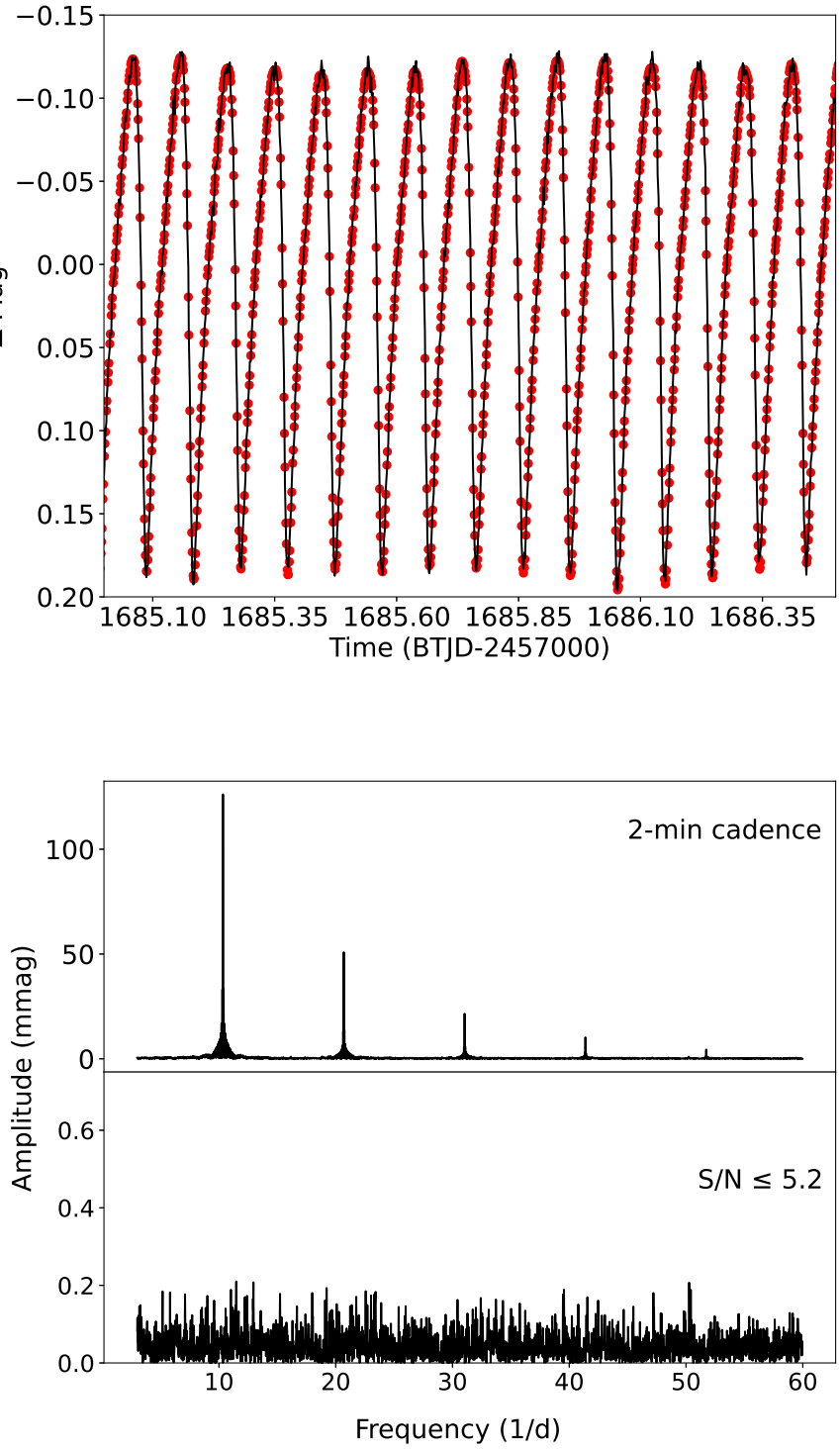

Figure 6. The short cadence light curve of TIC 160120432 during 1.5 days (top panel), power spectrum (middle panel), and power spectrum's residuals with SNR less than 5.2 (bottom panel).

Table 6. A complete list of the 20 frequencies identified TIC 278119167 (denoted by f_i). The frequency resolution is about f_{res} = 0.053.

f_i	Frequency (d^{-1})	Amplitude (mmag)	phase (radians)	S/N	ID	period ratio	Q value
1	12.59±0.00002	176.27±0.1	0.59±0.0002	797.74	F1	0.76	0.023±0.002
2	25.18±0.00007	49.62±0.1	0.87±0.0006	565.91	2F1	-	-
3	37.77±0.0003	9.709±0.1	0.91±0.003	142.05	3F1	-	-
4	50.36±0.0006	5.382±0.1	0.02±0.005	95.015	4F1	-	-
5	15.671±0.002	1.545±0.1	0.46±0.01	15.85	F2	0.61	0.018±0.002
6	18.734±0.002	1.439±0.1	0.19±0.02	18.098	-	-	-
7	28.26±0.003	1.098±0.1	0.48±0.02	16.202	F1+F2	-	-
8	9.579±0.005	0.218±0.1	0.47±0.04	4.18	F0	-	0.031±0.003
9	31.323±0.005	0.7438±0.1	0.64±0.08	11.72	-	-	-

Table 7. A complete list of the 20 frequencies identified TIC 710783 (denoted by f_i). The frequency resolution is about f_{res} = 0.058.

f_i	Frequency (d^{-1})	Amplitude (mmag)	phase (radians)	S/N	ID	period ratio	Q value
1	12.74±0.00005	164.6±0.4	0.463±0.0003	738.43	F0	-	0.039±0.003
2	25.48±0.0001	57.8±0.4	0.828±0.001	350.83	2F0	-	-
3	38.23±0.0004	19.72±0.4	0.291±0.03	126.32	3F0	-	-
4	50.97±0.001	7.89±0.4	0.922±0.008	68.48	4F0	-	-
5	7.25±0.003	2.82±0.4	0.899±0.02	10.83	-	-	-
6	36.27±0.003	2.74±0.4	0.182±0.02	22.87	-	-	-
7	5.48±0.003	2.42±0.4	0.737±0.02	7.88	-	-	-
8	32.74±0.003	2.32±0.4	0.372±0.02	18.55		-	-
9	54.50±0.006	1.43±0.4	0.635±0.04	11.05	-	-	-
10	18.23±0.008	1.02±0.4	0.743±0.06	8.35	-	-	-
11	11.83±0.009	0.91±0.4	0.763±0.07	5.44	-	-	-

stars' light curve (Table 6), which includes three independent frequencies F0 = 9.50 d^{-1} (P0 = 0.105 days), F1 = 12.590 d^{-1} and F2 = 15.671 d^{-1}, with Q values as 0.031, 0.023 and 0.018 respectively. Other frequencies may be represented as harmonics (f_2, f_3, f_4), combination frequencies (f_7), and non-radial modes (f_6,f_9). Again, in this star, the amplitude modulation phenomenon is probable due to the first overtone's amplitude being more significant than the fundamental frequency's amplitude (Bowman et al. 2016; Lv et al. 2021; Sun et al. 2021). Consequently, further studies are necessary to illuminate the driving mechanisms and mode selecting processes, which are still not fully understood in δ Sct stars. The rectified light curve shows a peak-to-peak amplitude of about ~ 0.43 mag, which may be suggested as a new triple-mode HADS.

4.6. *TIC 710783*

Figure 8 represents the light curve (top panel), power spectrum (middle panel), and power spectrum's residuals (bottom panel) for TIC 710783 (ATO J074.1485-27.6801) star. The TIC 710783 ($RA = 04^h56^m35.6357294103^s$, $DE = -27^h40^m48.564092138^s$) was first recognized as a variable star by Heinze et al. (2018), and then its physical parameters (temperature, gravity, and frequency scaling relation) were measured by Barceló Forteza et al. (2021) as δ Sct star. We suggest that TIC 710783 shows signs of a single-mode HADS. The *TESS* space telescope recorded TIC 710783 during sector 55 for 25.43 days and consisting of 17023 data points. We identified 11 frequencies constructing stars' light curve (Table 7), which includes an independent frequency F0 = 12.74 d^{-1} (P0 = 0.078 days), with Q value as 0.039. We observed the harmonics frequencies (f_2, f_3, f_4) and non-radial modes (f_5,f_6,...,f_{11}). The light curve's peak-to-peak value of about ~ 0.47 mag and the range of frequencies propose that TIC 710783 may be a new mono-mode HADS.

4.7. *TIC 187386415*

Figure 9 represents the light curve (top panel), power spectrum (middle panel), and power spectrum's residuals (bottom panel) for TIC 187386415 (ATO J236.5561-00.4351) star. TIC 187386415 ($RA = 15^h46^m13.482^s$, $DE = -00^h26^m06.345^s$) was classified

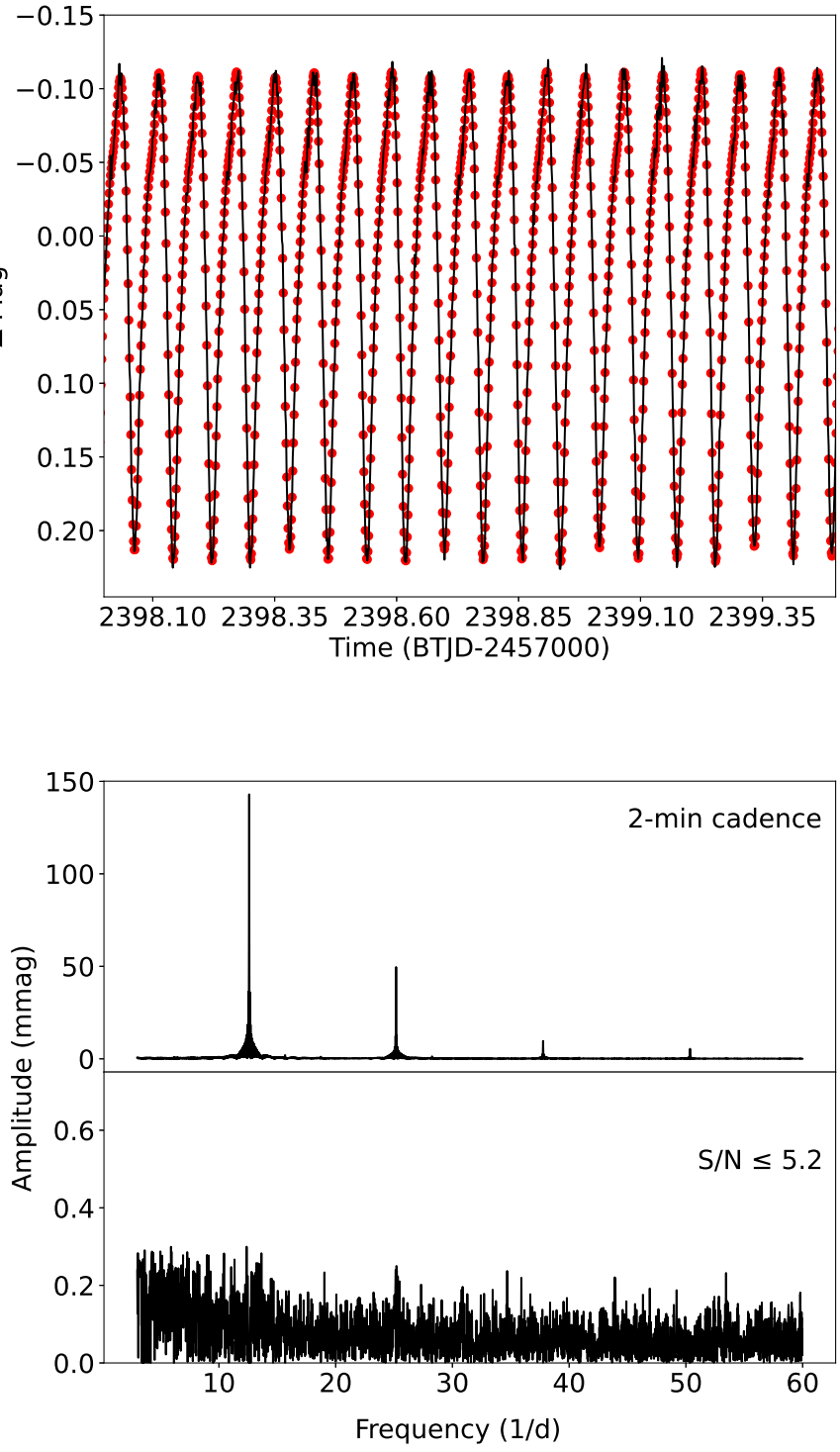

Figure 7. The short cadence light curve of TIC 278119167 during 1.5 days (top panel), power spectrum (middle panel), and power spectrum's residuals with SNR less than 5.2 (bottom panel).

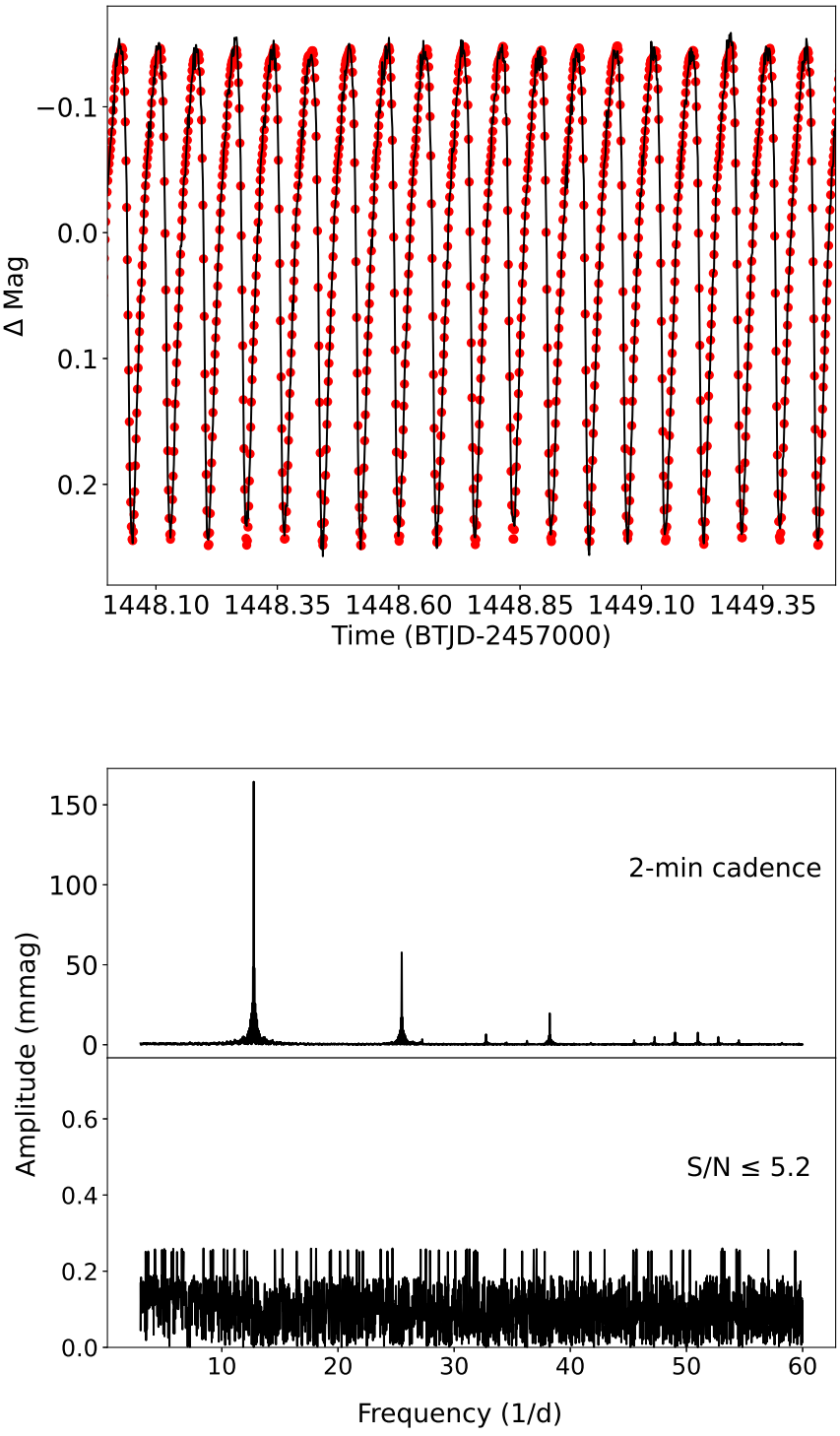

Figure 8. The short cadence light curve of TIC 710783 during 1.5 days (top panel), power spectrum (middle panel), and power spectrum's residuals with SNR less than 5.2 (bottom panel).

Table 8. A complete list of the 20 frequencies identified TIC 187386415 (denoted by f_i). The frequency resolution is about f_{res} = 0.078.

f_i	Frequency (d^{-1})	Amplitude (mmag)	phase (radians)	S/N	ID	period ratio	Q value
1	14.49±0.00003	113.88±0.1	0.551±0.0001	473.8	F0	-	0.033±0.0045
2	28.98±0.00009	41.077±0.1	0.868±0.0005	333.91	2F0	-	-
3	43.48±0.0002	15.634±0.1	0.223±0.001	196.24	3F0	-	-
4	57.97±0.0005	7.506±0.1	0.989±0.003	93.54	4F0	-	-

by Hey et al. (2021) as a variable star. This study shows that TIC 187386415 is a single-mode HADS. We analyzed this star for sector 51 with a duration of 19.13 days and consisting of 6775 data points. We identified four frequencies constructing stars' light curve (Table 8), which includes an independent frequency F0 = 14.49 d^{-1} (P0 = 0.069 days), with Q value as 0.033. Other frequencies may be introduced as harmonic frequencies (f_2, f_3, f_4). The peak-to-peak amplitude ($\sim$ 0.31 mag), and the frequencies' ranging that TIC 187386415 may be proposed as a new mono-mode HADS star.

4.8. *Asteroseismical parameters vs. physical quantities*

Using the Equation 3, we obtained the absolute magnitudes for seven HADS stars. We calculated the period (P0) of each star using the fundamental frequency (Tables 2-8). Figure 10 (Left panel) shows the PL relation for our HADS stars (colored star markers), the PL relation of Equation 5 (solid black), Equation 6 (red dashed line), and Equation 7 (cyan dash-dotted line). For stars, TIC 374753270 and TIC 130474019, the fundamental period and absolute magnitude agreed with Barac et al. (2022). As shown in Figure 10, all seven cases satisfy the PL relation for δ Sct stars that, indicates the validity of our frequency analysis.
Figure 10 (Right panel) examines the first and second overtone periods of TIC 278119167 by PL relations for the first (dashed line) and second (dotted line) overtones. The PL relation for the first and second overtones was obtained by Poro et al. (2021). While the TIC 278119167 star's fundamental period (shown as the largest star marker) slightly deviates from the fundamental PL relation, the first overtone period (the middle-size star marker) and the second overtone period (the smallest star marker) entirely agree with the first and second overtone PL relations. This implies the validity of the identified fundamental frequency for TIC 278119167.
Stellar metallicity is the abundance of heavier elements to hydrogen and helium. However, In astrophysics, it refers to the iron-to-hydrogen ratio ([Fe/H]) (Kotoneva et al. 2002; Chruslinska & Nelemans 2019). Netzel & Smolec (2022) obtained the [Fe/H] for 176 HADS stars by applying the MESA, Warsaw code, and optimization procedure. Using the mass (M), luminosity (L), fundamental period (P0), and the effective temperature ($T_{\rm eff}$) of these 176 HADS stars, we determined the following scaling relation for [Fe/H] as,

$$[\mathrm{Fe/H}]_s = \log_{10}\left(\left(\frac{M}{M_\odot}\right)^{7.95}\left(\frac{L}{L_\odot}\right)^{-1.83}\left(\frac{\mathrm{P0(day)}}{0.064}\right)^{0.79}\left(\frac{T_{\rm eff}}{K}\right)^{0.047}\right), \quad (8)$$

where $[\mathrm{Fe/H}]_s$ is the scaling metallicity obtained by an optimization procedure for 176 HADS stars. Figure 11 shows the comparison of [Fe/H] and scaling $[\mathrm{Fe/H}]_s$ (Equation 8) for HADS stars. Using Equation (8) we obtained the $[\mathrm{Fe/H}]_s$ of our seven newly identified HADS stars. We estimated the metallicity ranging from -0.47 dex to 0.28 dex (Table 9) for these seven HADS stars. The four HADS stars (TIC 374753270, TIC 148357344, TIC 160120432, and TIC 278119167) show a low iron abundance than the Sun, while the rest three HADS (TIC 130474019, TIC 710783, and TIC 187386415) demonstrating the positive [Fe/H]. The metallicities of these seven HADS stars are more significant than -0.5 dex indicating the metal-rich behavior (McNamara 2011). The metal-rich behavior is an essential characteristic of the evolved old stars.

5. CONCLUSION

To probe the new HADS stars from recent *TESS* observations of δ Sct stars, we recognized seven new targets, namely TIC 374753270, TIC 13047401, TIC 148357344, TIC 160120432, TIC 278119167, TIC 71083, and TIC 187386415 showing the peak-to-peak amplitude slightly more significant than 0.3 mag in their light curves. Using Equation 3, the *Gaia* DR3 parallaxes, the V-band absolute magnitude was calculated for these seven stars. Applying the *TESS* effective temperatures from Stassun et al. (2018) and the obtained absolute magnitudes, these seven HADS stars were located in the HR diagram. They lie in the δ Sct stars' stability strip of the HR diagram (Figure 2) close to the cooler boundary.
The HADS stars were expected to show a simple power spectrum, including one to a few large amplitudes. The period ratios, Q values and PL relation between the fundamental radial frequency and luminosity were used to show the validity of mode

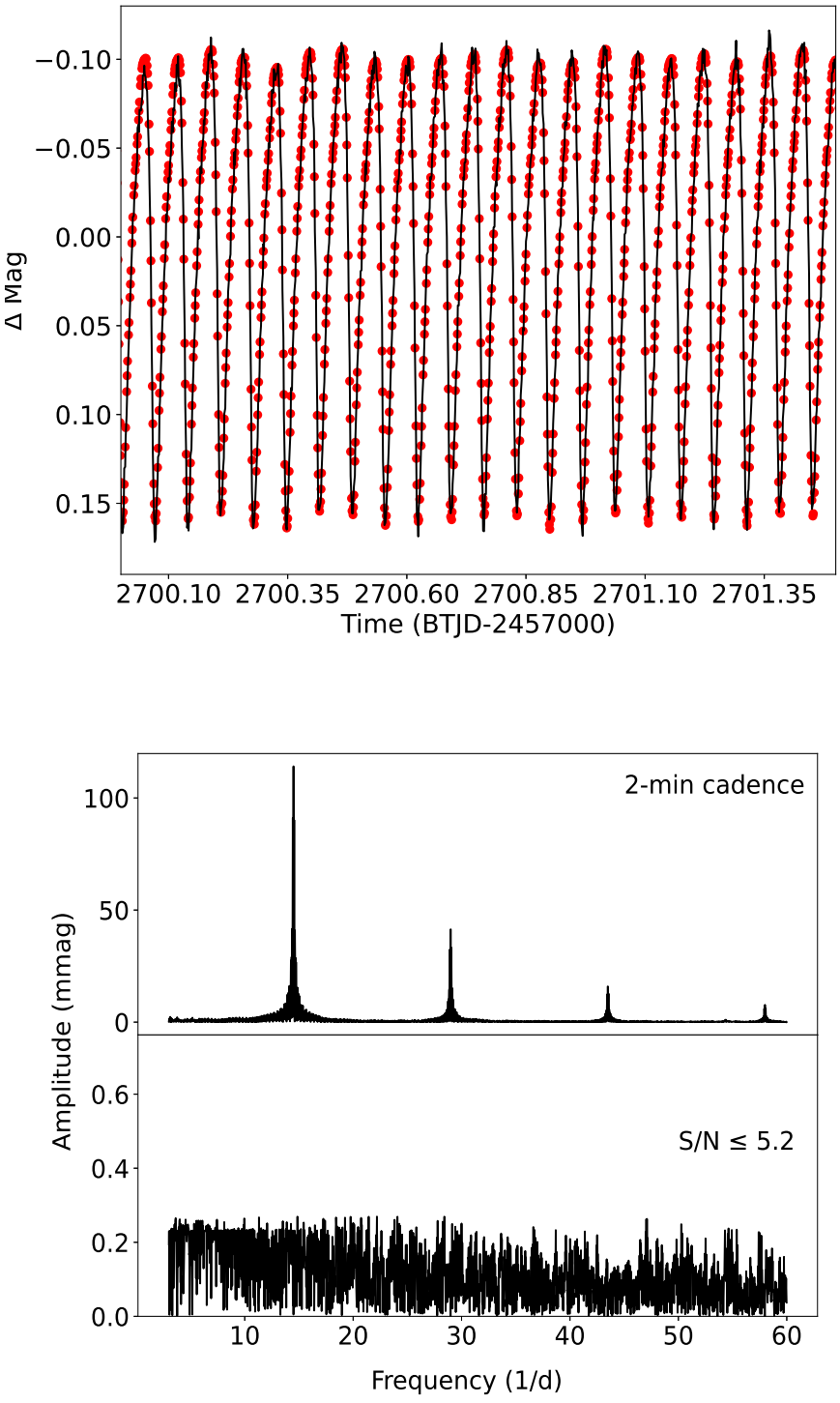

Figure 9. The short cadence light curve of TIC 187386415 during 1.5 days (top panel), power spectrum (middle panel), and power spectrum's residuals with SNR less than 5.2 (bottom panel).

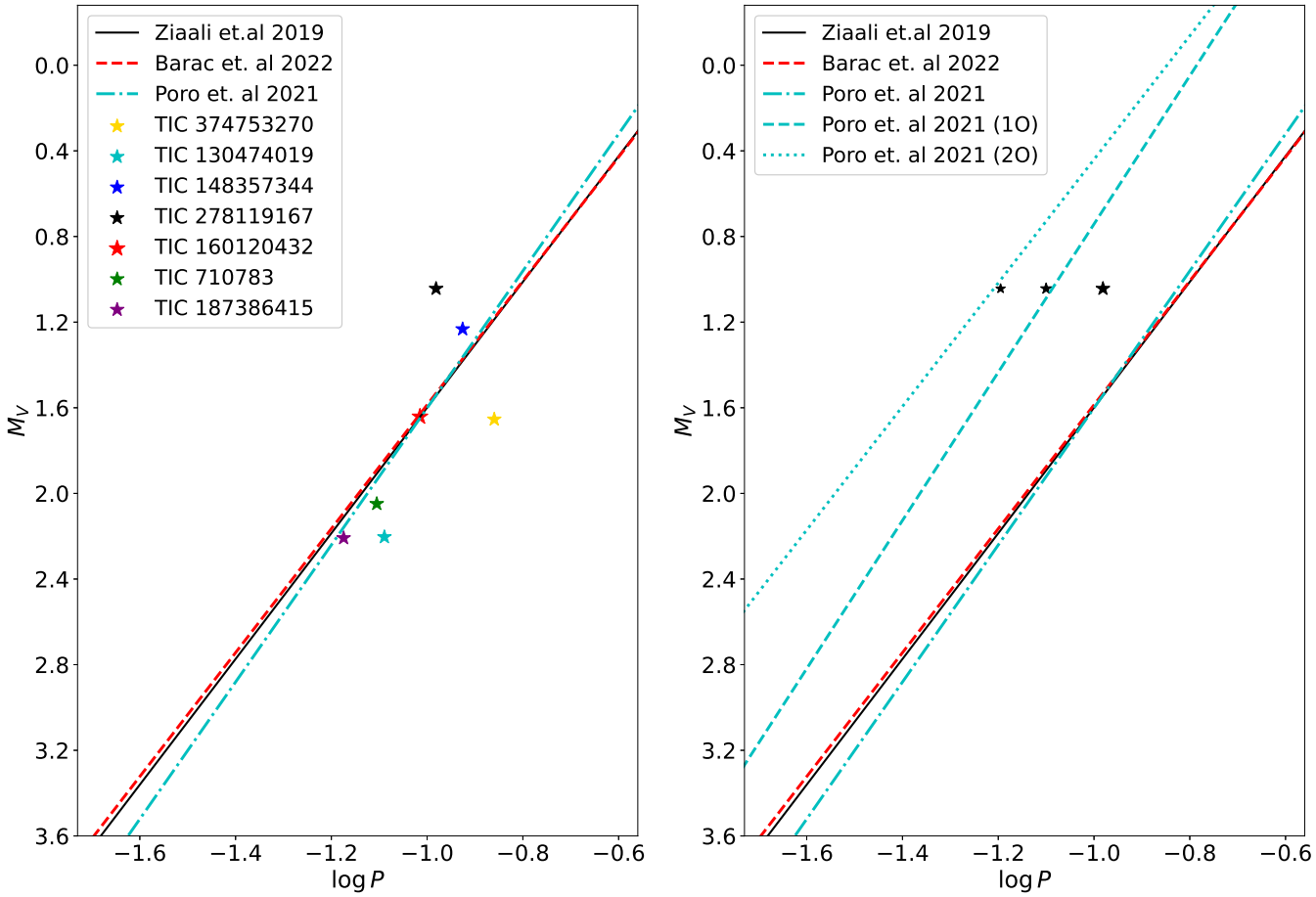

Figure 10. (Left panel) The period-luminosity (PL) diagram of our HADS stars (colored star markers). The solid black line shows the relation from Ziaali et al. (2019) (see Equation 5). The diagonal dashed red line shows the relation from Barac et al. (2022) (see Equation 6). The cyan dash–dotted line shows the relation from Poro et al. (2021) (see Equation 7). (Right panel) The PL relation of TIC 278119167 for the first (cyan dashed line) and second (cyan dotted line) overtones. While the fundamental mode (the largest star marker) slightly deviates from fundamental lines, the first (the middle-size star marker) and second (the smallest star marker) overtones are entirely consistent with their PL relations.

Table 9. TIC number, mass ($M/M_\odot$), radius ($R/R_\odot$), surface gravity (log g), effective temperature ($T_{\rm eff}$), luminosity ($L/L_\odot$), *TESS* magnitude, highest peak frequency ($f_{A_{max}}$), absolute V-band magnitude ($M_{\rm V}$), and metallicity ([Fe/H]$_{\rm s}$) for seven HADS stars.

TIC number	$M/M_\odot$	$R/R_\odot$	log g (dex)	$T_{\rm eff}$ (K)	$L/L_\odot$	*TESS* mag	$f_{A_{max}}$ (d^{-1})	$M_{\rm V}$	[Fe/H]$_{\rm s}$ (dex)
374753270	1.60	3.043	3.67552	7166	21.88	10.712	7.24	1.61	-0.413
130474019	1.76	1.93	4.1123	7573	11.04	11.9773	12.28	2.2	0.284
148357344	1.610	2.999	3.69103	7183	21.72	11.9665	11.09	1.51	-0.428
160120432	1.590	2.510	3.8402	7138	14.68	11.7877	10.35	1.614	-0.228
278119167	1.680	2.681	3.8068	7369	19.0	12.042	12.59	1.056	-0.232
710783	1.770	1.924	4.11758	7604	11.14	12.6615	12.74	2.048	0.278
187386415	1.670	1.939	4.08548	7340.63	9.83	12.086	14.94	2.208	0.137

information for these seven stars. We applied the frequency spectrum diagram to achieve the harmonic information of these stars, and we accepted the mode characteristics (frequencies, amplitudes, and phases) that followed a signal-to-noise ratio (SNR) greater than 5.2. Our analyses show that the HADS stars were categorized into single-modes (TIC 374753270, TIC 710783, and TIC 187386415), double-modes (TIC 130474019 and TIC 160120432), and triple-modes (TIC 148357344 and TIC 278119167). We determined the variety of harmonic and combination frequencies in the power spectrum of targets (Tables 2 to 8) as well as

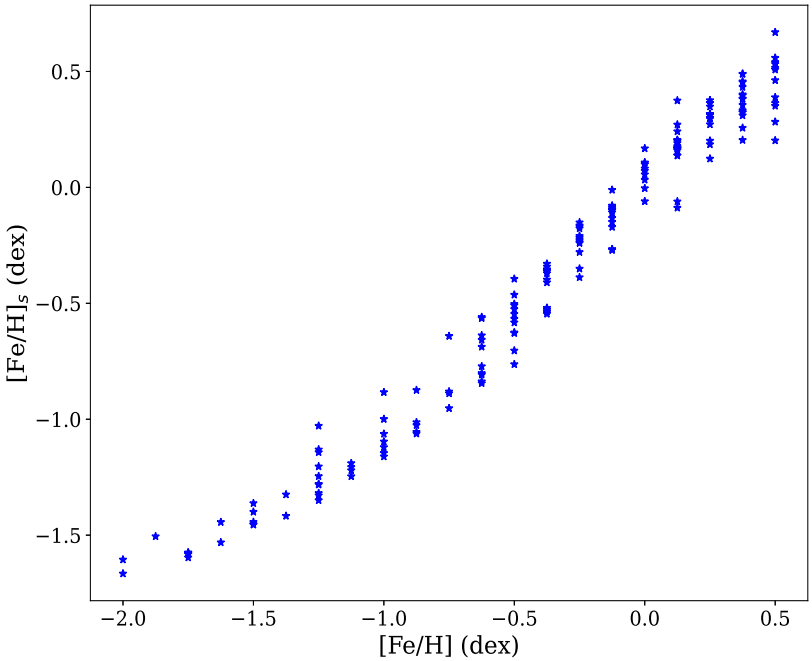

Figure 11. The scaling metallicity $[Fe/H]_s$ (Equation 8) versus the metallicity [Fe/H] for 176 HADS stars (Netzel & Smolec 2022).

non-radial oscillation frequencies for most of our targets. We derived a scaling relation using 176 HADS stars from Netzel & Smolec (2022) between metallicity ([Fe/H]) and physical parameters (mass (M), luminosity (L), and the effective temperature ($T_{\rm eff}$)) and fundamental period (P0). Using Equation 8, we estimated the metallicity of the seven HADS stars. The metallicity for TIC 374753270, TIC 130474019, TIC 148357344, TIC 160120432, TIC 278119167, TIC 710783, and TIC 187386415 were estimated to be -0.413, 0.284, -0.428, -0.228, -0.232, 0.278, and 0.137 in dex unit, respectively.

6. ACKNOWLEDGMENTS

This manuscript includes data collected by the *TESS* mission, which are publicly available from the Mikulski Archive for Space Telescopes (MAST). Funding for the *TESS* mission is provided by the NASA Explorer Program. Funding for the *TESS* Asteroseismic Science Operations Centre is provided by the Danish National Research Foundation (Grant agreement no.: DNRF106), ESA PRODEX (PEA 4000119301), and Stellar Astrophysics Centre (SAC) at Aarhus University. We would like to thank the *Gaia* team for providing accurate data from the European Space Agency (ESA) mission *Gaia*, processed by the *Gaia* Data Processing and Analysis Consortium (DPAC). Funding for the DPAC has been provided by national institutions, in particular, the institutions participating in the *Gaia* Multilateral Agreement. Also, this work has been entirely supported by the Iran National Science Foundation (INSF) under grant No. 4002562. E.Ziaali expresses her gratitude for that.

REFERENCES

1997, ESA Special Publication, Vol. 1200, The HIPPARCOS and TYCHO catalogues. Astrometric and photometric star catalogues derived from the ESA HIPPARCOS Space Astrometry Mission

Aerts, C., Christensen-Dalsgaard, J., & Kurtz, D. W. 2010, Asteroseismology (Springer Netherlands), doi: 10.1007/978-1-4020-5803-5

Aguirre, V. S., Davies, G. R., Basu, S., et al. 2015, Monthly Notices of the Royal Astronomical Society, 452, 2127, doi: 10.1093/mnras/stv1388

Antoci, V. 2014, in Precision Asteroseismology, ed. J. A. Guzik, W. J. Chaplin, G. Handler, & A. Pigulski, Vol. 301, 333–340, doi: 10.1017/S1743921313014543

Antoci, V., Handler, G., Campante, T. L., et al. 2011, Nature, 477, 570, doi: 10.1038/nature10389

Antoci, V., Cunha, M. S., Bowman, D. M., et al. 2019, MNRAS, 490, 4040, doi: 10.1093/mnras/stz2787

Baker, N., & Kippenhahn, R. 1962, ZA, 54, 114

Balmforth, N. J., & Gough, D. O. 1990, ApJ, 362, 256, doi: 10.1086/169262

Barac, N., Bedding, T. R., Murphy, S. J., & Hey, D. R. 2022, MNRAS, doi: 10.1093/mnras/stac2132

Baran, A. S., Koen, C., & Pokrzywka, B. 2015, MNRAS, 448, L16, doi: 10.1093/mnrasl/slu194

Barceló Forteza, S., Moya, A., Barrado, D., et al. 2020, A&A, 638, A59, doi: 10.1051/0004-6361/201937262

Barceló Forteza, S., Moya, A., Barrado, D., et al. 2021, in The 20.5th Cambridge Workshop on Cool Stars, Stellar Systems, and the Sun (CS20.5), Cambridge Workshop on Cool Stars, Stellar Systems, and the Sun, 136, doi: 10.5281/zenodo.4564172

Barclay, T., Pepper, J., & Quintana, E. V. 2018, ApJS, 239, 2, doi: 10.3847/1538-4365/aae3e9

Bedding, T. R., Murphy, S. J., Hey, D. R., et al. 2020, Nature, 581, 147, doi: 10.1038/s41586-020-2226-8

Bono, G., Caputo, F., Cassisi, S., et al. 1997, ApJ, 477, 346, doi: 10.1086/303710

Bowman, D. M. 2017, Amplitude Modulation of Pulsation Modes in Delta Scuti Stars (Springer), doi: 10.1007/978-3-319-66649-5

Bowman, D. M., Kurtz, D. W., Breger, M., Murphy, S. J., & Holdsworth, D. L. 2016, MNRAS, 460, 1970, doi: 10.1093/mnras/stw1153

Bowman, D. M., & Michielsen, M. 2021, Astronomy amp; Astrophysics, 656, A158, doi: 10.1051/0004-6361/202141726

Breger, M. 1979, Publications of the Astronomical Society of the Pacific, 91, 5, doi: 10.1086/130433

Breger, M. 1990, in Astronomical Society of the Pacific Conference Series, Vol. 11, Confrontation Between Stellar Pulsation and Evolution, ed. C. Cacciari & G. Clementini, 263–273

Breger, M. 2000a, in Astronomical Society of the Pacific Conference Series, Vol. 210, Delta Scuti and Related Stars, ed. M. Breger & M. Montgomery, 3

Breger, M. 2000b, MNRAS, 313, 129, doi: 10.1046/j.1365-8711.2000.03185.x

Breger, M., & Bregman, J. N. 1975, ApJ, 200, 343, doi: 10.1086/153794

Breger, M., Balona, L., Lenz, P., et al. 2011, Monthly Notices of the Royal Astronomical Society, 414, 1721, doi: 10.1111/j.1365-2966.2011.18508.x

Chang, S. W., Protopapas, P., Kim, D. W., & Byun, Y. I. 2013, AJ, 145, 132, doi: 10.1088/0004-6256/145/5/132

Chruslinska, M., & Nelemans, G. 2019, Monthly Notices of the Royal Astronomical Society, 488, 5300, doi: 10.1093/mnras/stz2057

Dékány, I., & Grebel, E. K. 2022, ApJS, 261, 33, doi: 10.3847/1538-4365/ac74ba

Dupret, M. A., Grigahcène, A., Garrido, R., Gabriel, M., & Scuflaire, R. 2005, A&A, 435, 927, doi: 10.1051/0004-6361:20041817

Gilliland, R. L., Brown, T. M., Christensen-Dalsgaard, J., et al. 2010, PASP, 122, 131, doi: 10.1086/650399

Green, G. M., Schlafly, E. F., Finkbeiner, D., et al. 2018, MNRAS, 478, 651, doi: 10.1093/mnras/sty1008

Guzik, J. A. 2021, Frontiers in Astronomy and Space Sciences, 8, 55, doi: 10.3389/fspas.2021.653558

Handler, G. 2009, in American Institute of Physics Conference Series, Vol. 1170, Stellar Pulsation: Challenges for Theory and Observation, ed. J. A. Guzik & P. A. Bradley, 403–409, doi: 10.1063/1.3246528

Hasanzadeh, A., Safari, H., & Ghasemi, H. 2021, MNRAS, 505, 1476, doi: 10.1093/mnras/stab1411

Heinze, A. N., Tonry, J. L., Denneau, L., et al. 2018, AJ, 156, 241, doi: 10.3847/1538-3881/aae47f

Hey, D. R., Montet, B. T., Pope, B. J. S., Murphy, S. J., & Bedding, T. R. 2021, AJ, 162, 204, doi: 10.3847/1538-3881/ac1b9b

Holdsworth, D. L., Cunha, M. S., Lares-Martiz, M., et al. 2024, MNRAS, 527, 9548, doi: 10.1093/mnras/stad3800

Houdek, G., Balmforth, N. J., Christensen-Dalsgaard, J., & Gough, D. O. 1999, A&A, 351, 582, doi: 10.48550/arXiv.astro-ph/9909107

Jayasinghe, T., Stanek, K. Z., Kochanek, C. S., et al. 2020, MNRAS, 493, 4186, doi: 10.1093/mnras/staa499

Jenkins, J. M., Twicken, J. D., McCauliff, S., et al. 2016, in Society of Photo-Optical Instrumentation Engineers (SPIE) Conference Series, Vol. 9913, Software and Cyberinfrastructure for Astronomy IV, ed. G. Chiozzi & J. C. Guzman, 99133E, doi: 10.1117/12.2233418

Kotoneva, E., Flynn, C., & Jimenez, R. 2002, Monthly Notices of the Royal Astronomical Society, 335, 1147, doi: 10.1046/j.1365-8711.2002.05690.x

Leavitt, H. S., & Pickering, E. C. 1912, Harvard College Observatory Circular, 173, 1

Lenz, P., & Breger, M. 2005, Communications in Asteroseismology, 146, 53, doi: 10.1553/cia146s53

Li, X.-Y., Huang, Y., Liu, G.-C., Beers, T. C., & Zhang, H.-W. 2023, The Astrophysical Journal, 944, 88, doi: 10.3847/1538-4357/acadd5

Liakos, A., & Niarchos, P. 2017, MNRAS, 465, 1181, doi: 10.1093/mnras/stw2756

Lianou, S., Grebel, E. K., & Koch, A. 2011, A&A, 531, A152, doi: 10.1051/0004-6361/201116998

Lightkurve Collaboration, Cardoso, J. V. d. M., Hedges, C., et al. 2018, Lightkurve: Kepler and TESS time series analysis in Python, Astrophysics Source Code Library, record ascl:1812.013. http://ascl.net/1812.013

Liu, G. C., Huang, Y., Zhang, H. W., et al. 2020, ApJS, 247, 68, doi: 10.3847/1538-4365/ab72f8

Loumos, G. L., & Deeming, T. J. 1978, Ap&SS, 56, 285, doi: 10.1007/BF01879560

Lv, C., Esamdin, A., Hasanzadeh, A., et al. 2023, The Astrophysical Journal, 959, 33, doi: 10.3847/1538-4357/acf999

Lv, C., Esamdin, A., Pascual-Granado, J., Yang, T., & Shen, D. 2022, ApJ, 932, 42, doi: 10.3847/1538-4357/ac69d9

Lv, C., Esamdin, A., Zeng, X., et al. 2021, The Astronomical Journal, 162, 48, doi: 10.3847/1538-3881/ac082b

McNamara, D. H. 2011, AJ, 142, 110, doi: 10.1088/0004-6256/142/4/110

Milligan, H., & Carson, T. R. 1992, Ap&SS, 189, 181, doi: 10.1007/BF00643125

Montgomery, M. H., & O'Donoghue, D. 1999, Delta Scuti Star Newsletter, 13, 28

Mow, B., Reinhart, E., Nhim, S., & Watkins, R. 2016, AJ, 152, 17, doi: 10.3847/0004-6256/152/1/17

Murphy, S. J., Hey, D., Van Reeth, T., & Bedding, T. R. 2019, MNRAS, 485, 2380, doi: 10.1093/mnras/stz590

Murphy, S. J., Saio, H., Takada-Hidai, M., et al. 2020, MNRAS, 498, 4272, doi: 10.1093/mnras/staa2667

Netzel, H., & Smolec, R. 2022, MNRAS, 515, 4574, doi: 10.1093/mnras/stac1938

Otero, S. A. 2007, Open European Journal on Variable Stars, 0056, 1

Petersen, J. O., & Christensen-Dalsgaard, J. 1996, A&A, 312, 463

Pietrukowicz, P., Soszyński, I., Netzel, H., et al. 2020, AcA, 70, 241, doi: 10.32023/0001-5237/70.4.1

Poro, A., Paki, E., Mazhari, G., et al. 2021, PASP, 133, 084201, doi: 10.1088/1538-3873/ac12dc

Read, A. K., Bedding, T. R., Mani, P., et al. 2024, arXiv e-prints, arXiv:2401.07413, doi: 10.48550/arXiv.2401.07413

Ricker, G. R., Winn, J. N., Vanderspek, R., et al. 2015, Journal of Astronomical Telescopes, Instruments, and Systems, 1, 014003, doi: 10.1117/1.JATIS.1.1.014003

Samadi, R., Goupil, M. J., & Houdek, G. 2002, A&A, 395, 563, doi: 10.1051/0004-6361:20021322

Soszyński, I., Pietrukowicz, P., Skowron, J., et al. 2021, AcA, 71, 189, doi: 10.32023/0001-5237/71.3.1

Stassun, K. G., Oelkers, R. J., Pepper, J., et al. 2018, AJ, 156, 102, doi: 10.3847/1538-3881/aad050

Stellingwerf, R. F. 1979, ApJ, 227, 935, doi: 10.1086/156802

Sun, X.-Y., Zuo, Z.-Y., Yang, T.-Z., Chen, X.-H., & Li, H.-R. 2021, The Astrophysical Journal, 922, 199, doi: 10.3847/1538-4357/ac323e

Uytterhoeven, K., Moya, A., Grigahcène, A., et al. 2011, A&A, 534, A125, doi: 10.1051/0004-6361/201117368

Wils, P., Rozakis, I., Kleidis, S., Hambsch, F. J., & Bernhard, K. 2008, A&A, 478, 865, doi: 10.1051/0004-6361:20078992

Xue, W., Niu, J.-S., Xue, H.-F., & Yin, S. 2023, Research in Astronomy and Astrophysics, 23, 075002, doi: 10.1088/1674-4527/accdbc

Yang, T.-Z., Sun, X.-Y., Zuo, Z.-Y., & Liu, H.-W. 2021a, AJ, 161, 27, doi: 10.3847/1538-3881/abcb8b

Yang, T.-Z., Zuo, Z.-Y., Li, G., et al. 2021b, A&A, 655, A63, doi: 10.1051/0004-6361/202142198

Ziaali, E., Bedding, T. R., Murphy, S. J., Reeth, T. V., & Hey, D. R. 2019, Monthly Notices of the Royal Astronomical Society, 486, 4348, doi: 10.1093/mnras/stz1110